Determination of the elemental composition of geological rocks and minerals by the method of tagged neutrons

Alexakhin V.Y. Bystritskii V.M., Zamyatin N.I., Zubarev E.V., Krasnopyorov A.V., Rapacki V.L., Rogachev A.V., Rogov Yu.N., A.B. Sadovsky, Salmin R.A., M.G. Sapozhnikov, Slepnev V.M., S.V. Khabarov, Razinkov E.A. and Tarasov O.G.
Joint Institute for Nuclear Research, Dubna,
"Diamant" LLC, Dubna

Sklyarov E.V.
Institute of the Earth's Crust SB RAS, Irkutsk

A.V. Lavrenchuk
Institute of Geology and Mineralogy SB RAS, Novosibirsk

Introduction

The main purpose of the measurements was to check the possibility of the tagged neutron method (TNM) to perform rapid analysis of the elemental composition of rocks from a relatively homogeneous by reference elements groups.

For example, separation of carbonate rocks:

- calcite marble (without magnesium)
- dolomite and dolomite-calcite marbles (with a substantial share of magnesium)
- calciphyres (rock with a substantial admixture of silicates and varying ratios of calcium and magnesium)

It was interesting to see how well the TNM results are correlated with the results of petrographic analysis carried out in the field, and how well they correlate with the results of chemical analysis in the laboratory.

Tagged neutron method (TNM)

Initially was used by us for the detection of hidden explosives. Prompt gamma produced by 14 MeV neutron inelastic reactions with nuclei $n + A \rightarrow n' + A^*$. Fast neutrons are produced in the $d + T \rightarrow^4 He + n$ reaction. Tagging is done by segmented alpha-detector.

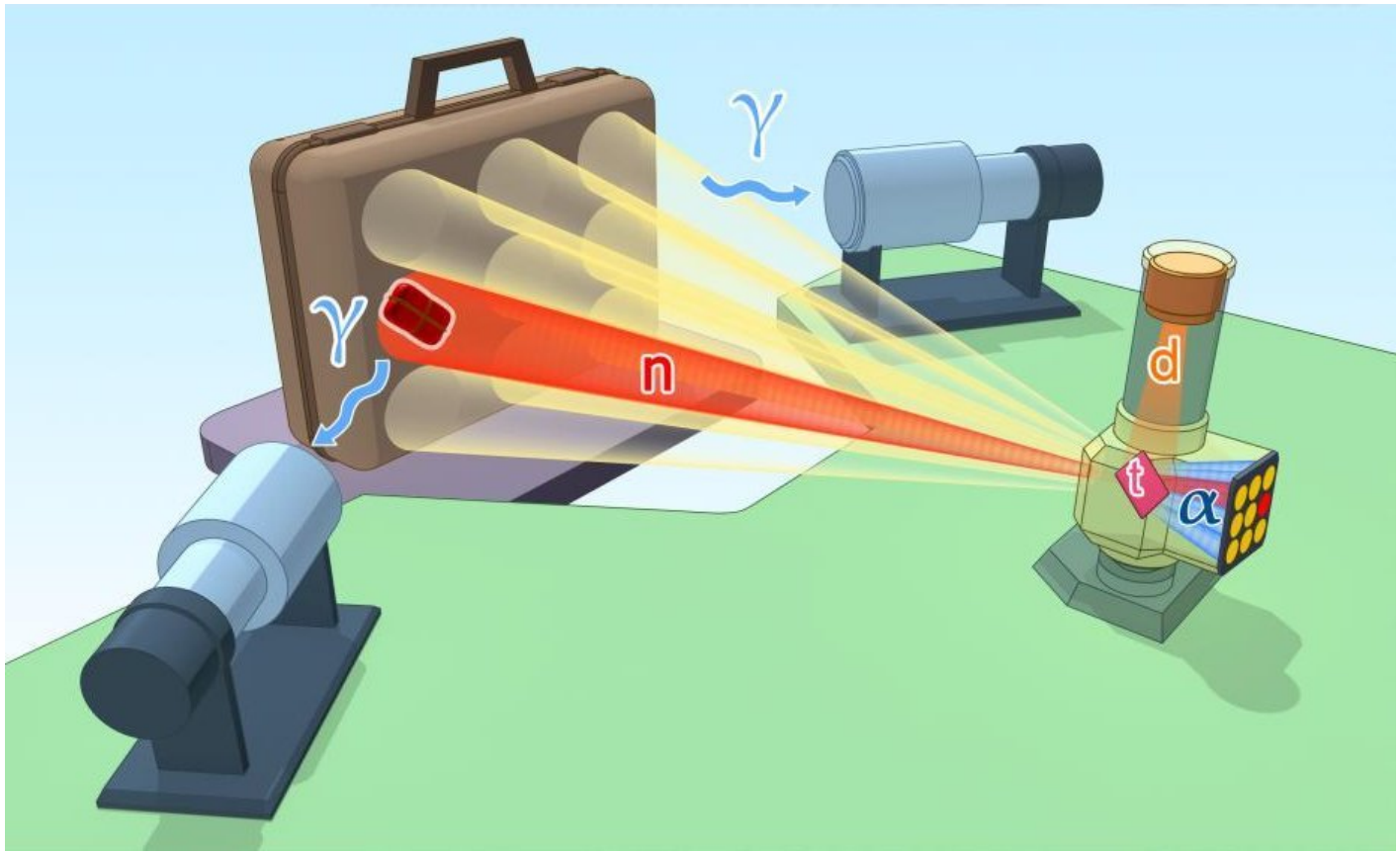

Advantages of neutron tagging

800g of melamine ($C_3H_6N_6$)

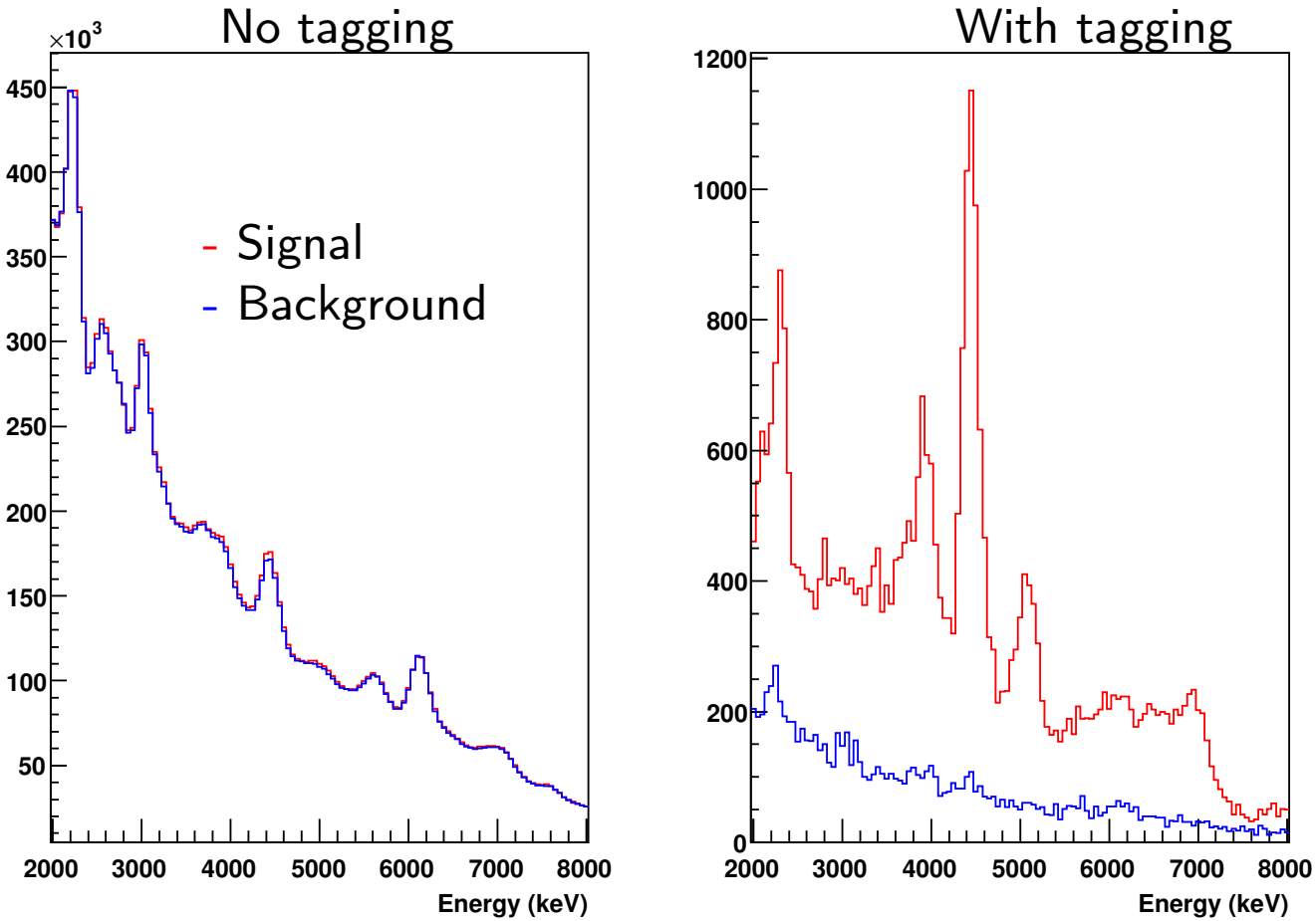

Tagging of neutron allows to improve signal to background ratio on the factor of 200-400. Tagging allows to do 3D scan of the sample.

Portable detector of explosives DVIN-1

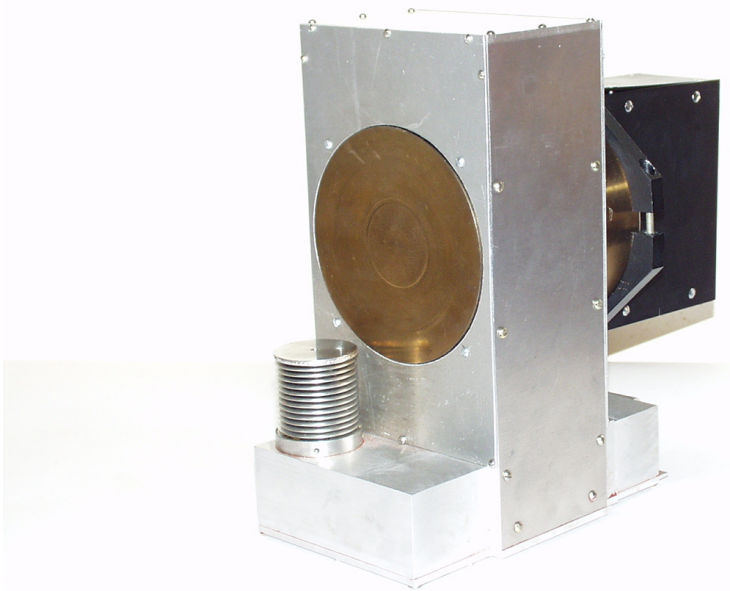

- For detection of hidden explosives.
- Size 74x51x41 cm and its weight is 40 kg.
- Measures C, N, O in the substance.
- Portable neutron generator ING-27 (VNIIA)with a built-in-9-alpha-pixel detector. $I_{NG} = 5 \cdot 10^7 \text{sec}^{-1}$
- DAQ and power supplies.
- 76x65 mm BGO gamma detector. $\sigma_E/E = 4.4\%$ for $E_\gamma = 4.44$ MeV.
- Time resolution $(\alpha - \gamma)$-coincidences 3.3 ns.
- Measures C, N, O in the substance.

Gamma-spectra of elements

- Different elements have different gamma spectra
- The total spectrum of the substance can be decomposed
- Measured 24 elements C, N, O, F, Na, Mg, Al, Si, P, S, Cl, K, Ca, Ti, Cr, Mn, Fe, Ni, Cu, Zn, Zr, Sn, Pb, Bi.

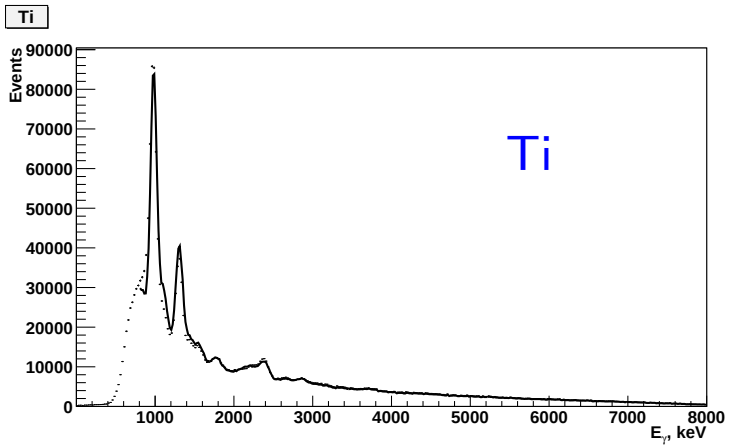

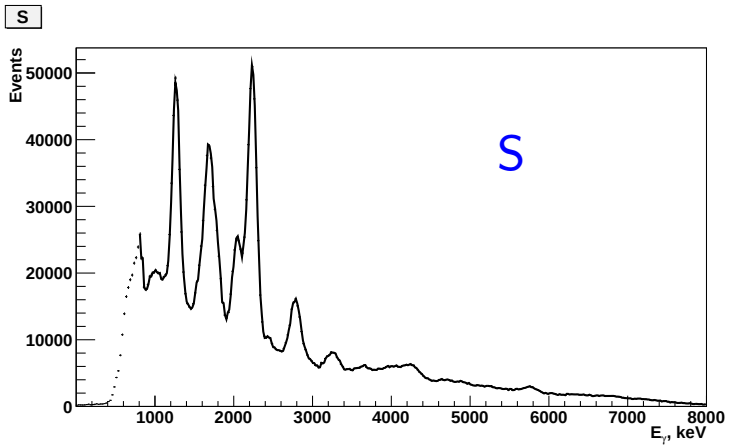

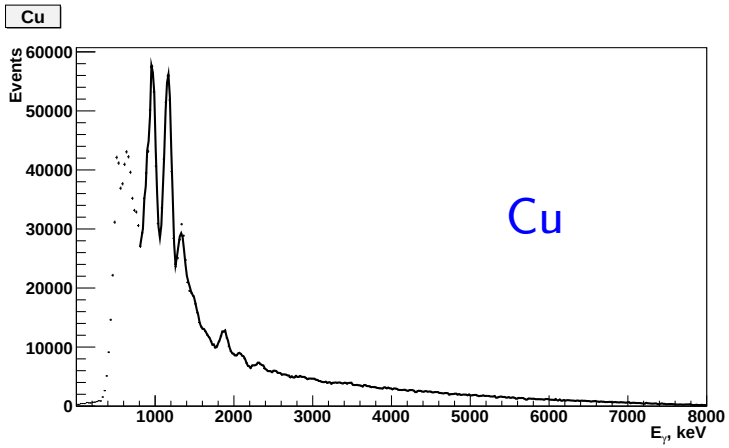

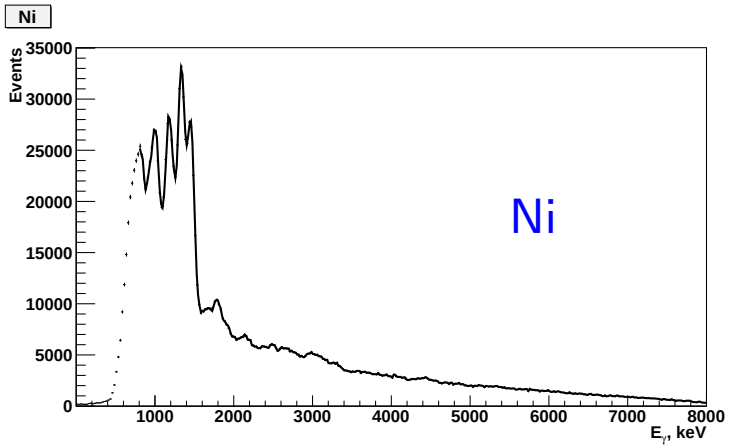

Determination of elemental composition

For one element the number of gamma rays entering the detector N_f is

$$N_f = \frac{N_{in}\sigma N_{Av}\rho l W}{A},$$

N_{in} - number of neutrons incident on the target, σ - total cross section of the reaction $(n, n'\gamma)$, N_{Av} - Avogadro's number, ρ - target density, l -target length, A - atomic weight of the element, W - the probability of gamma ray detection.

For the case of a target consisting of various elements j:

$$N_f = N_{in} l \rho W \sum_j n_j \sigma_j$$

σ_j - cross section for the element j, n_j - the number of nuclei of element j in the target.

By measuring the spectrum of gamma rays and knowing the gamma production cross sections σ_j for different elements one can restore the relative proportions of the elements in the target.

Fit function (I)

Fit function for all elements $j = C, O, Si, Mg, Ca, Fe, Al$ is as follows (parameters of the fit are in bold):

$$S(E) = \sum_{j=C,O,Si...} (\mathbf{N_j} \sum_{i=1}^{i=k_j} \sigma_{ij} P_{ij}(E) \epsilon_{ph}(E_i) + Cont_j(E)) + Bg(E)$$

k_j - number of peaks for the element j, P_{ij} - fit function (response function) for gamma-line i with energy E_i, $\mathbf{N_j}$ - parameter which determines the amount of the element j in the spectrum , σ_{ij} - cross section of the gamma ray with the energy E_{ij}. $Cont_j(E)$ - amplitude of the " Continuum spectrum". Since the production cross section σ_{ij} and total absorption peak efficiency(included in the P_{ij}) are given, the normalization of the element is determined by a single parameter $\mathbf{N_j}$. $Bg(E)$ - function of the "background". $\epsilon_{ph}(E_i)$ - total absorption peak efficiency for the energy E_i (from MC).

Fit function (II)

Fit function (response function) for gamma-line with energy E_i are as follows (parameters of the fit are in bold):

$$P_i(E) = \frac{1}{\sqrt{2\pi}\sigma_{\mathbf{i}}^{\mathbf{ph}}} G(E_i, \sigma_{\mathbf{i}}^{\mathbf{ph}}) + \frac{\mathbf{R_0} r^{es}(E_i)}{\sqrt{2\pi}\sigma_i^{es}} G(E_i - 511, \sigma_i^{es}) + \frac{\mathbf{R_0} r^{es}(E_i) r^{es2}(E_i)}{\sqrt{2\pi}\sigma_i^{es2}} G(E_i - 1022, \sigma_i^{es2}) + N_i^c \mathbf{R_{Compt}} C(E_i, E)$$

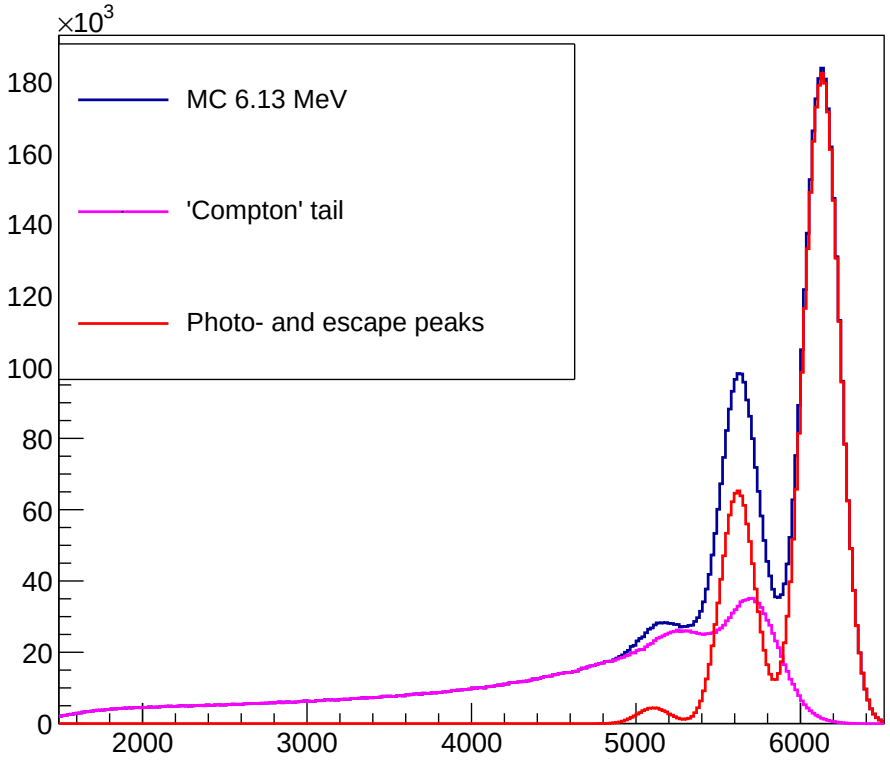

- $\sigma_{\mathbf{i}}^{\mathbf{ph}}$ - the energy resolution (depends as $\sqrt{E}$).
- $r^{es}(E)$ and $r^{es2}(E_i)$ - define the amplitudes of escape peaks, normalized relatively to the amplitude of the photopeak. Dependence from the energy is set by MC, but $\mathbf{R_0}$ is used to adjust them.
- $C(E_i, E)$ - Compton "tail" function.
- $\mathbf{R_{Compt}}$ - factor to adjust Compton "tail" amplitude.
- $G(\overline{x}, \sigma)$ -Gauss function.

Spectrum of oxygen

Gamma lines ^{16}O. For the case $E_\gamma > 1MeV$.

H_2O

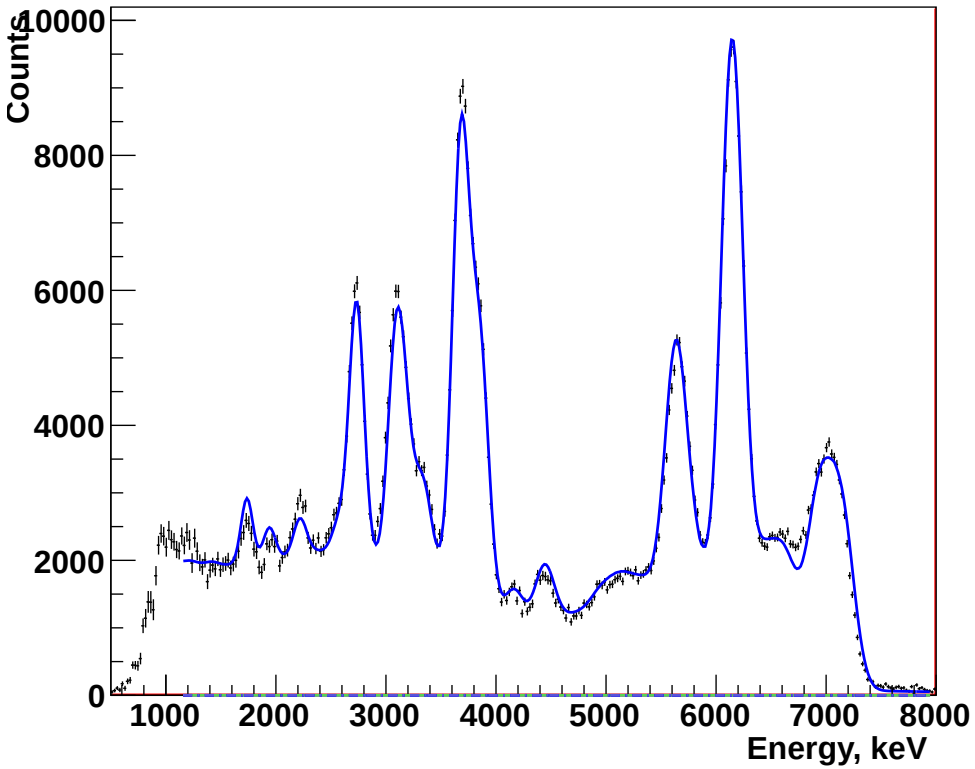

E_γ keV	σ mBarn	process
7117	52	$(n, n')^{16}O$
6917	51	$(n, n')^{16}O$
6130	146	$(n, n')^{16}O$
4950	3	$(n, n')^{16}O$
4438	10	$(n, n'\alpha)^{12}C$
4163	6	$(n, n')^{16}O$
3854	37.8	$(n, \alpha)^{13}C$
3840	5.8	$(n, n')^{16}O$
3685	85	$(n, \alpha)^{13}C$
3089	25.6	$(n, \alpha)^{13}C$
2742	30	$(n, n')^{16}O$
1955	3.	$(n, n')^{16}O$
1755	5.	$(n, n')^{16}O$

Spectrum of Si

Gamma lines ^{28}Si. For the case $E_\gamma > 1MeV$.

E_γ keV	σ mBarn	process
^{12}C 4438	200	$(n, n')^{12}C$

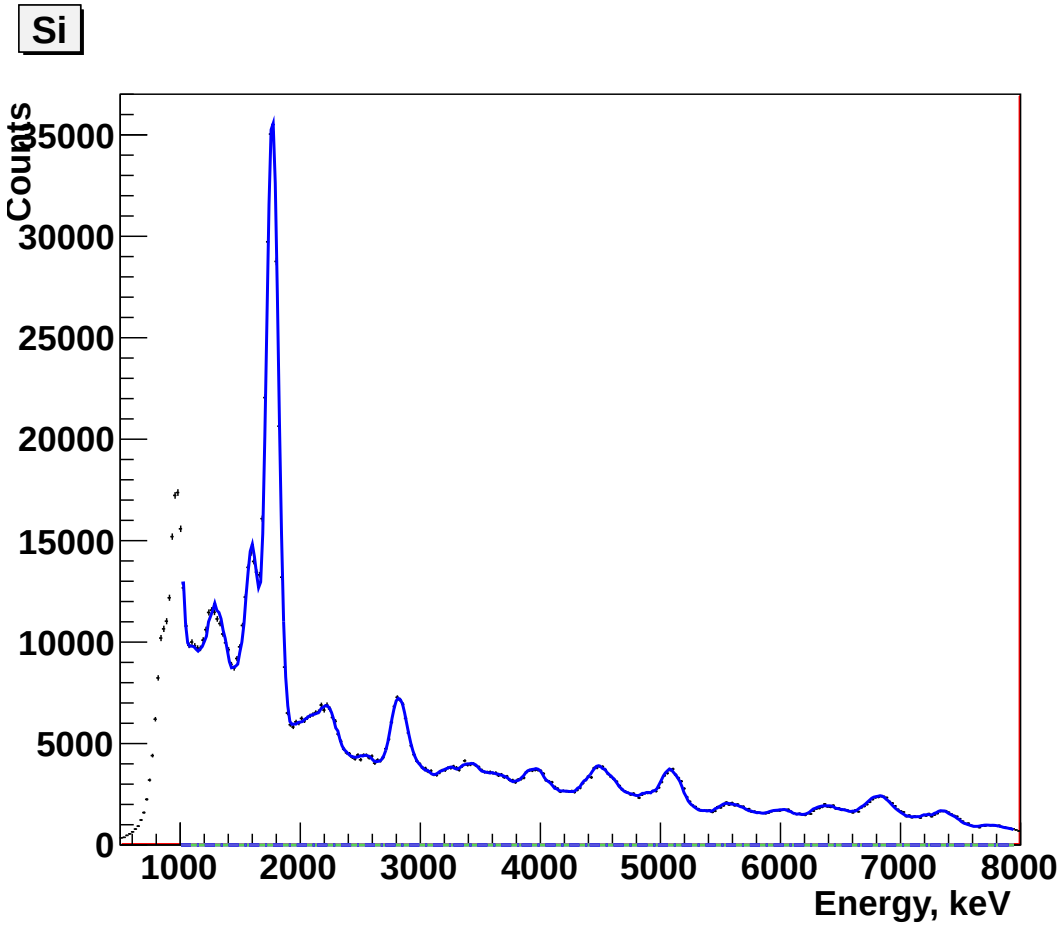

E_γ keV	σ mBarn	process
7816	16.2	$(n, n')^{28}Si$
7415.2	8.7	$(n, n')^{28}Si$
7379.5	26.8	$(n, n')^{28}Si$
6877.88	28.7	$(n, n')^{28}Si$
5600.95	15.6	$(n, n')^{28}Si$
5108.11	59.0	$(n, n')^{28}Si$
4496.8	28.5	$(n, n')^{28}Si$
3925.4	19.6	$(n, n')^{28}Si$
3640.6	13.8	$(n, n')^{28}Si$
3430	14.6	$(n, p)^{28}Al?$
3278	10.0	$(n, n')^{28}Si$
2838.67	62.0	$(n, n')^{28}Si$
2240	32.7	$(n, p)^{28}Al?$
2100	5.6	$(n, p)^{28}Al?$
2052.1	13.4	$(n, n')^{28}Si$
1779	325.0	$(n, n')^{28}Si$
1599	79.4	$(n, p)^{28}Al$
1375	12.6	$(n, p)^{28}Al?$
1280	17.0	$(n, p)^{28}Al?$

Spectrum of Mg

Gamma lines Mg. For the case $E_\gamma > 1MeV$ and $\sigma > 4$ mBarn

Mg

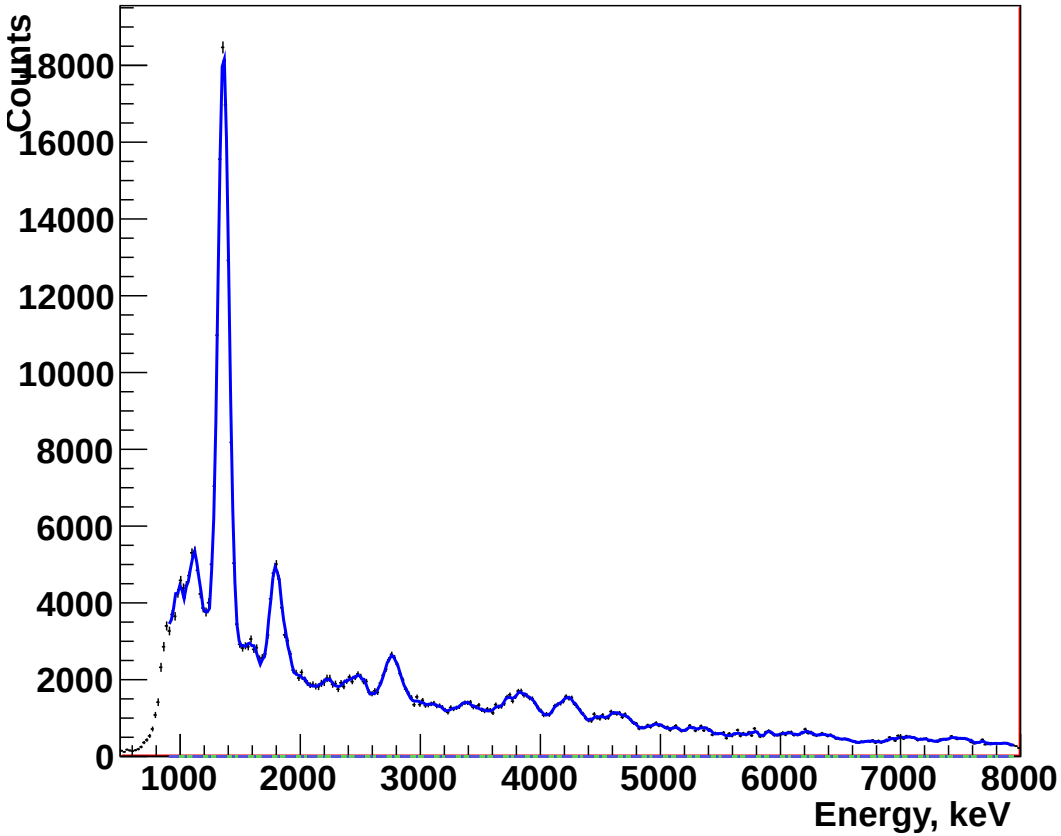

E_γ keV	σ mBarn	process
4640	26.2	$(n, n')^{24}Mg$
4239	40.7.	$(n, n')^{24}Mg$
3867	39.9.	$(n, n')^{24}Mg$
2770	60.7	$(n, n')^{24}Mg$
2520	22.4	$(n, n')^{24}Mg$?
1809	70.2	$(n, n')^{26}Mg$
1610	13.0	$(n, n')^{26}Mg$?
1369	353.3	$(n, n')^{24}Mg$
1130	28.3	$(n, n')^{24}Mg$

Spectrum of Al

Gamma lines Al. For the case $E_\gamma > 1MeV$ and $\sigma > 4$ mBarn

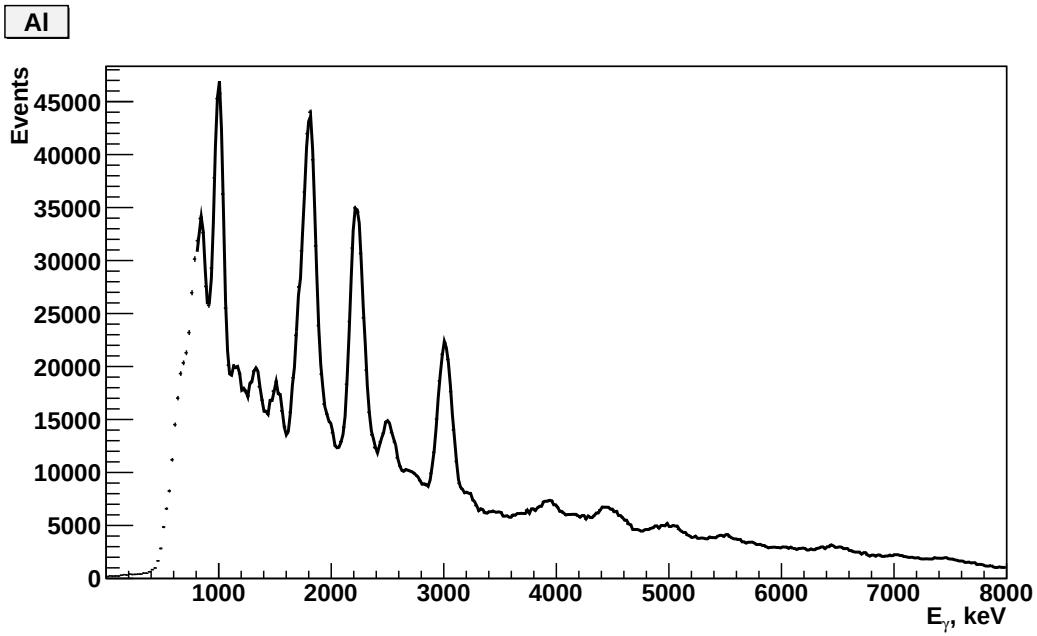

E_γ keV	σ mBarn	process
3203	9.3	$(n, n')^{27}Al$
3004	109.0	$(n, n')^{27}Al$
2231	139.5	$(n, n')^{27}Al$
1809	127.6	$(n, n')^{27}Al$
1720	11.8	$(n, n')^{27}Al$
1698	30.0	$(n, p)^{27}Mg$
1014	35.5	$(n, n')^{27}Al$
985	37.2	$(n, n')^{27}Al$?
844	28.7	$(n, n')^{27}Al$?

Silicium oxide

Check how it works on simple substances

The proportion by the number of atoms. Expected: Si: 0.33 0: 0.66 TNM: Si: 0.34 ± 0.01 O: 0.66 ± 0.01

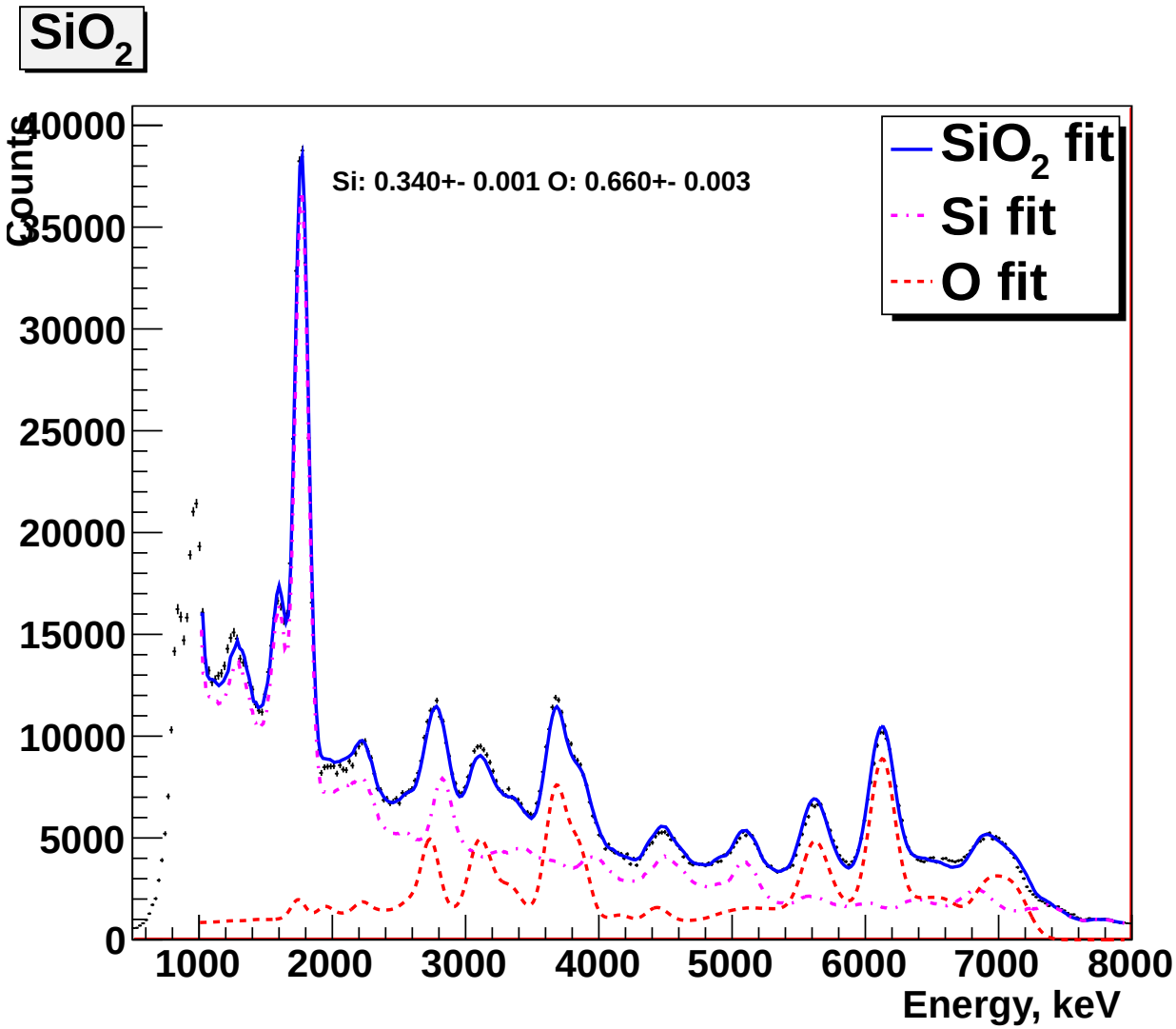

Determination of mass content of elements and oxides of the elements

Knowing the relative proportions of the elements in the sample N_j ($\sum_j N_j = 1$) it is possible to calculate the mass fractions of the elements in the sample as a

$$w_j = \frac{N_j m_j}{\sum_j N_j m_j}$$

where m_j - atomic weight of an element j.
To calculate the mass fractions of oxides of elements of W_j we define the mass fraction of the element j in the appropriate oxide $J_x O_y$ $\epsilon_j = \frac{x m_j}{x m_j + y m_O}$. Then

$$W_j = \frac{\frac{N_j m_j}{\epsilon_j}}{\sum_j \frac{N_j m_j}{\epsilon_j}}$$

Mass fraction (percentage by mass) of elements in the samples according to chemical analysis.
$w_i = \frac{m_i}{m_{tot}} \cdot 100\%$.

Chernorud

The second phase of research was carried out at Olkhon geodynamic testing ground at Chernorud (Irkutsk GTU). The cite is situated in 2km from the Lake Baikal and Olkhon island. The portable detector DVIN-1 was brought there and the irradiation of samples of different rocks was carried out.

Chernorud (II)

17 samples of marble, 23 samples of gneisses and 7 samples of amphibolites were irradiated. No special sample preparation was conducted. Sample size ranged from 20 to 50 cm, weight from 2 to 6 kg.

Samples (III)

The sample was placed at a distance of 15 cm from the exit window of DVIN-1 (32 cm from the tritium target). The distance from the sample to the gamma detectors was 20 cm. At this distance survey area was approximately 15x15 cm. It was divided into 9 areas (the number of tagged beams). The intensity of the neutron generator was $I = 5 \cdot 10^7 \text{sec}^{-1}$. Typical time of irradiation was 15 minutes.

The spectrum of calcite marble ($CaCO_3$)

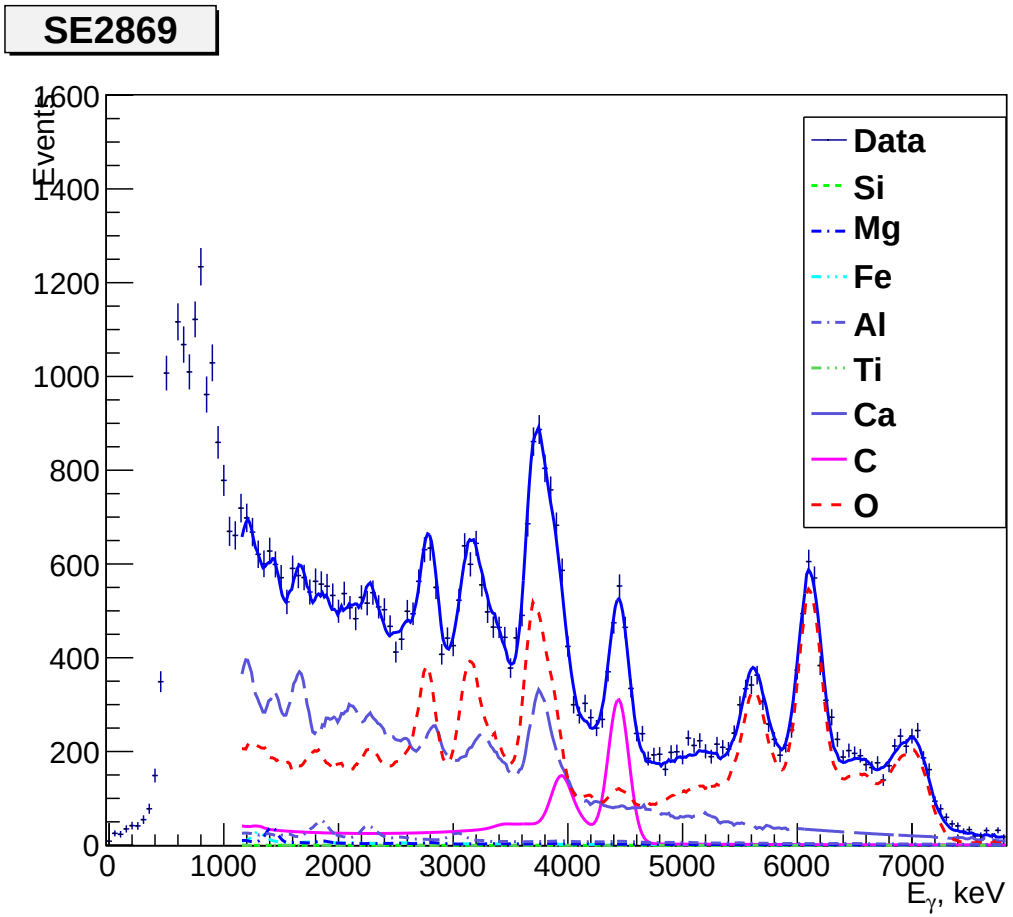

Mass fraction (percentage by mass) of the elements

	Si,%	Mg,%	Fe,%	Al,%	Ca,%	C,%	O,%
SE2869	-	-	-	2.6 ± 1.0	34.9 ± 1.8	13.2 ± 0.6	48.8 ± 1.4
SE2801	-	-	-	-	42.3 ± 1.3	16.1 ± 0.7	41.6 ± 1.2
SE2766A	1.0 ± 0.4	-	-	-	43.6 ± 1.7	13.2 ± 0.6	42.1 ± 1.1

The spectrum of dolomite ($CaCO_3$x$MgCO_3$)

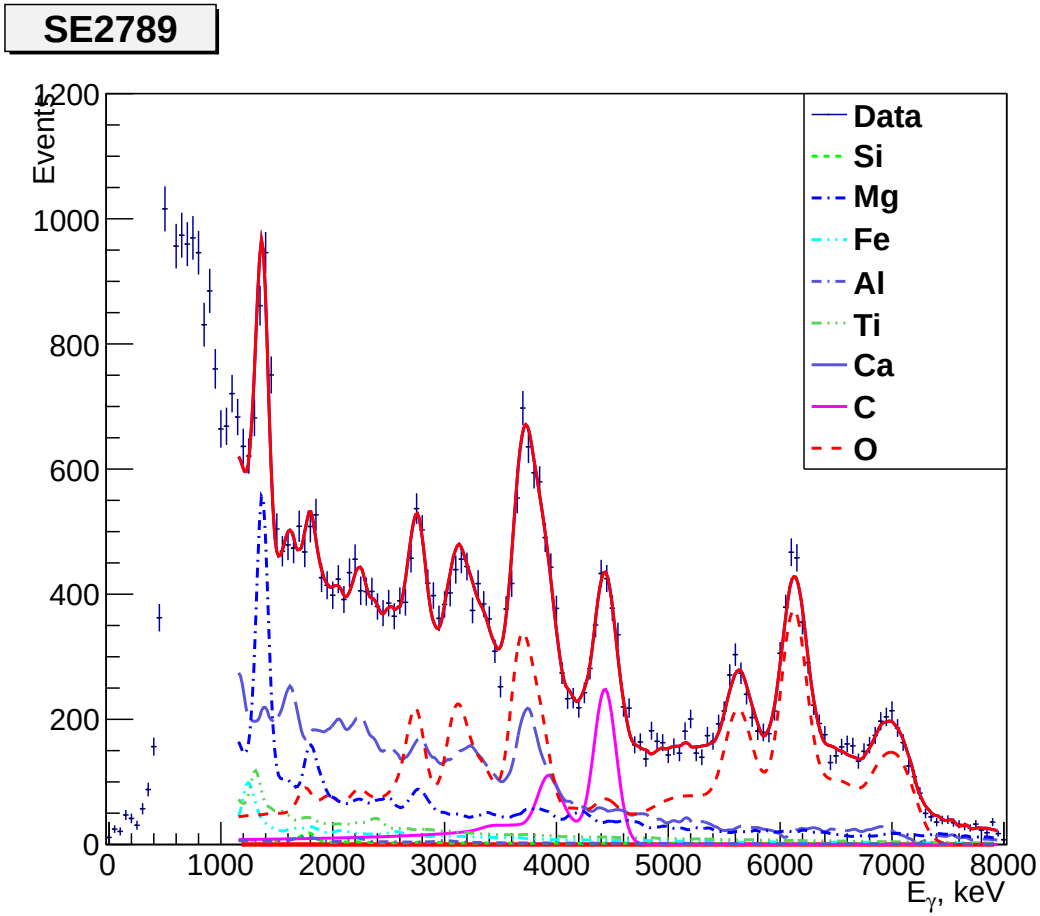

	Si,%	Mg,%	Fe,%	Al,%	Ca,%	C,%	O,%
SE2789	0.2 ± 0.8	9.6 ± 0.6	-	2.5 ± 1.0	27.5 ± 2.2	14.4 ± 0.7	45.3 ± 1.9
SE2871	0.5 ± 0.8	7.7 ± 0.6	2.1 ± 1.1	0.7 ± 1.1	25.3 ± 2.0	15.0 ± 0.7	48.8 ± 1.7
SE2842	-	8.9 ± 0.6	-	2.0 ± 0.8	28.3 ± 2.1	15.9 ± 0.8	44.6 ± 1.7

The spectrum of calciphyre.

Calcite or dolomite with a admixture of silicate materials

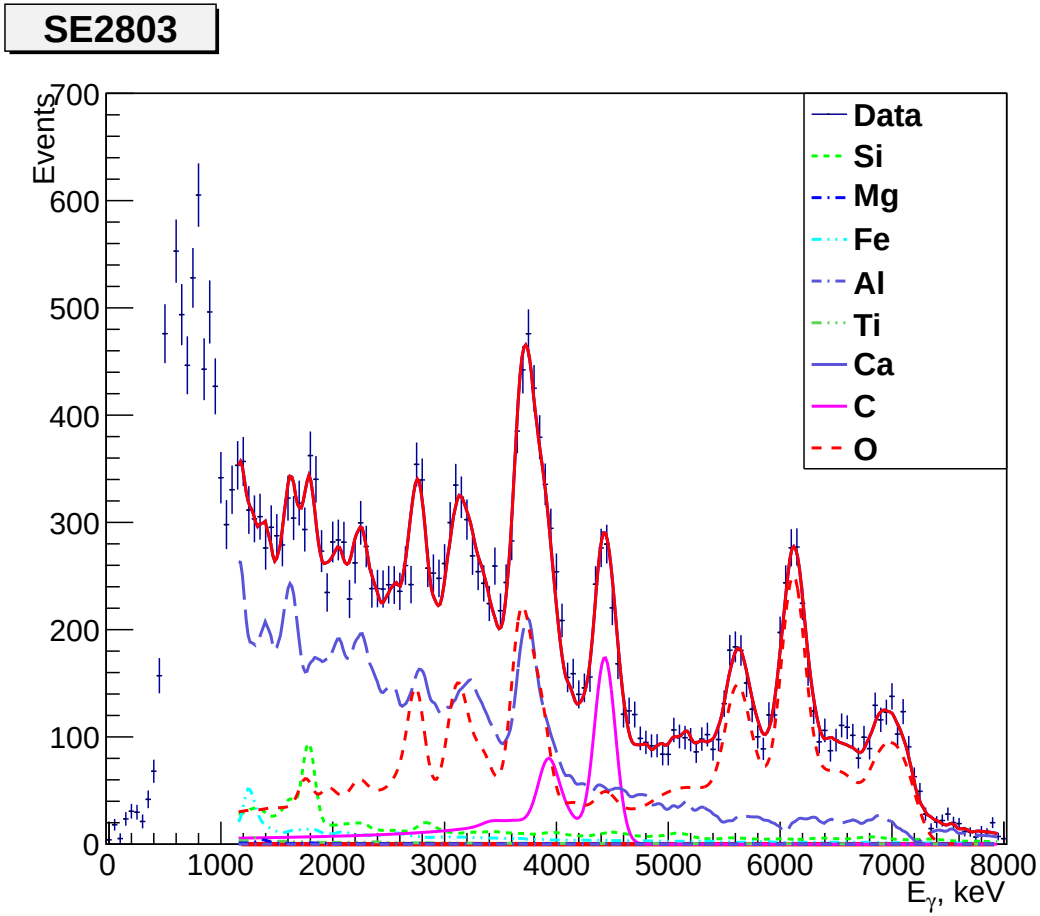

	Si,%	Mg,%	Fe,%	Al,%	Ca,%	C,%	O,%
SE2841	3.9 ± 0.9	-	-	-	40.2 ± 2.7	14.0 ± 0.8	39.9 ± 2.0
SE2803	2.9 ± 0.9	-	-	2.2 ± 1.4	39.6 ± 2.5	13.9 ± 0.8	41.4 ± 2.0
SE2794	3.0 ± 0.7	-	-	-	43.7 ± 1.2	14.2 ± 0.6	38.5 ± 0.9

The spectrum of gneiss

Mainly composed of SiO_2 and Al_2O_3

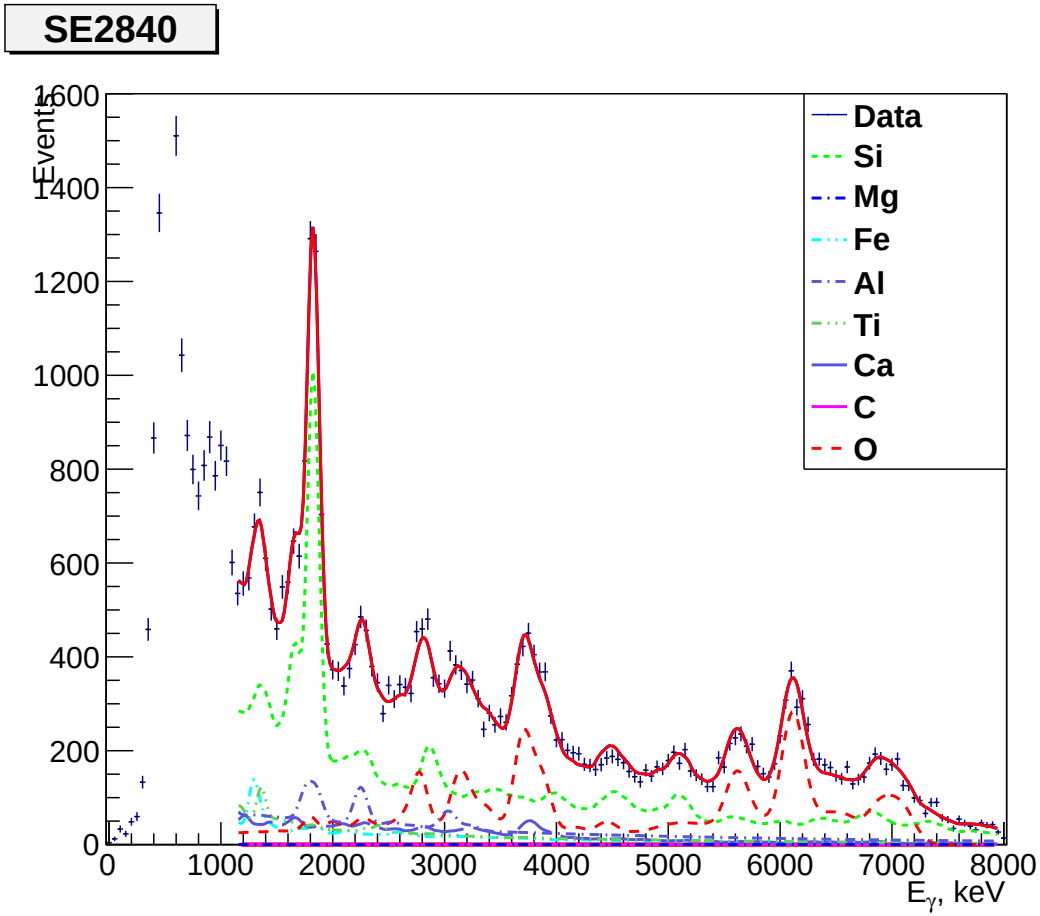

	Si,%	Mg,%	Fe,%	Al,%	Ca,%	C,%	O,%
SE2840	26.9 ± 1.5	6.7 ± 0.7	0.9 ± 1.3	16.4 ± 1.7	6.8 ± 2.4	-	42.4 ± 1.9
SE2870	33.1 ± 2.0	2.8 ± 0.8	1.6 ± 1.7	13.4 ± 2.2	0.8 ± 3.3	1.2 ± 0.8	47.1 ± 3.0
SE2786	32.1 ± 1.8	1.5 ± 0.6	4.7 ± 1.4	11.4 ± 1.6	6.5 ± 2.2	0.4 ± 0.6	43.7 ± 1.9

The spectrum of amphibolite

Composed mainly of silicates and aluminum silicates of magnesium, iron and calcium.

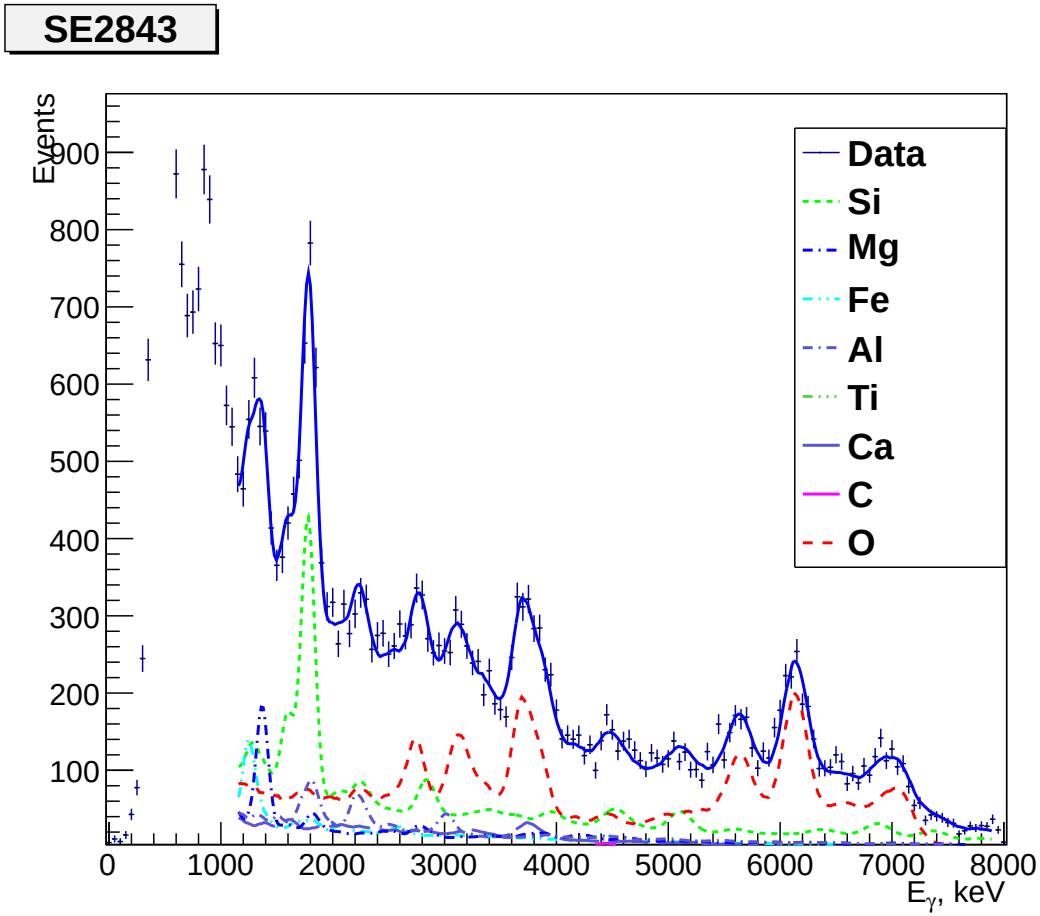

	Si,%	Mg,%	Fe,%	Al,%	Ca,%	C,%	O,%
SE2843	22.9 ± 2.0	6.0 ± 0.9	10.3 ± 2.1	7.8 ± 2.0	9.8 ± 4.7	-	42.6 ± 3.0
SE2850	17.6 ± 1.6	4.1 ± 0.7	9.9 ± 1.6	11.5 ± 1.7	15.3 ± 2.8	-	41.6 ± 2.7
SE2816	21.4 ± 1.61	4.7 ± 0.7	11.1 ± 1.7	10.7 ± 1.7	12.3 ± 2.7	-	39.0 ± 2.3

Comparison of the results

Mass fraction of oxides according to chemical analysis and as a result of fit procedure.

	SiO_2	MgO	FeO	Al_2O_3	CaO	CO_2
SE2843	47.16	6.66	11.69	15.67	10.97	0.44
SE2843 TNM	48.5 ± 4.4	8.2 ± 1.3	15.2 ± 2.3	13.8 ± 3.3	12.3 ± 4.0	2.0 ± 2.4
SE2869	2.29	0.68	0.	0.	53.35	42.3
SE2869 TNM	0.4 ± 1.4	0.3 ± 0.6	0.00 ± 0.6	4.8 ± 1.8	47.4 ± 2.8	47.2 ± 2.5
SE2870	73.16	0.81	2.79	13.34	2.38	0.
SE2870 TNM	65.4 ± 5.8	4.2 ± 1.3	1.9 ± 2.0	23.4 ± 4.0	1.0 ± 4.3	4.0 ± 2.8
SE2786	73.13	0.53	2.36	14.06	3.58	0.51
SE2786 TNM	62.7 ± 4.3	2.3 ± 0.8	5.5 ± 1.7	19.8 ± 2.9	8.3 ± 2.9	1.4 ± 2.1
SE2800	62.31	2.34	6.54	17.05	3.72	0.
SE2800 TNM	54.5 ± 3.9	5.4 ± 1.1	5.7 ± 1.9	21.0 ± 2.9	12.6 ± 3.2	0.9 ± 2.1
SE2801	1.1	0.65	0.12	0.	54.4	42.98
SE2801 TNM	0.0 ± 0.3	0.0 ± 0.1	0.0 ± 0.6	0.0 ± 0.8	50.1 ± 1.8	50.0 ± 2.3
SE2841	4.95	0.31	0.51	0.5	51.8	40.18
SE2841 TNM	6.7 ± 1.7	0.0 ± 1.1	1.0 ± 1.2	1.6 ± 2.1	47.3 ± 3.5	43.2 ± 2.9

Statistical errors can be improved by using all 9 beams

Conclusions

- Determination the elemental composition of rocks using the TNM was carried out in the field.
- The analysis of 47 samples of three groups of rocks was done: carbonate rocks (marbles and calciphyres), gneisses and amphibolites. For each sample the mass fractions of the elements O, Si, Mg, Ca, Fe, Al, and C were determined with an accuracy of few % by using only one tagged beam.
- The separation of calcite marble, dolomite and calciphyres as the result of the analysis is entirely consistent with the identified by mineralogical and petrographic characteristics.
- The method of tagged neutrons has good prospects for use in geological practice in the analysis of rock samples. The advantage of this method is its rapidity, absense of requirements for sample preparation, the ability to determine the elemental composition of rocks inside of a large thickness, the ability to determine the variations in the volume directly on the objects of prospecting or mining.
- We have obtained the base of the cross sections of the characteristic lines of gamma rays for 24 elements C, N, O, F, Na, Mg, Al, Si, P, S, Cl, K, Ca, Ti, Cr, Mn, Fe, Ni, Cu, Zn, Zr, Sn, Pb, Bi.

Additional slides

Additional slides

Advantages of tagged neutron method (TNM)

Compared with other methods of rapid analysis of the elemental composition of rocks, such as X-ray fluorescence analysis (XRF), TNM detector has the following advantages:

- Ability to determine the concentrations of light elements. For XRF it is difficult to determine the elements with Z <11. TNM well defines the concentration of light elements such as F, N, C, O.
- Large area screening. XRF instruments are inspection zone of a few millimeters. Area inspection detectors TNM is 30x30 cm at a distance of 60 cm. In addition it is possible to determine the distribution of the concentration of elements inside of the sample.
- Using TNM detector in the field requires no sample preparation.

The time distribution

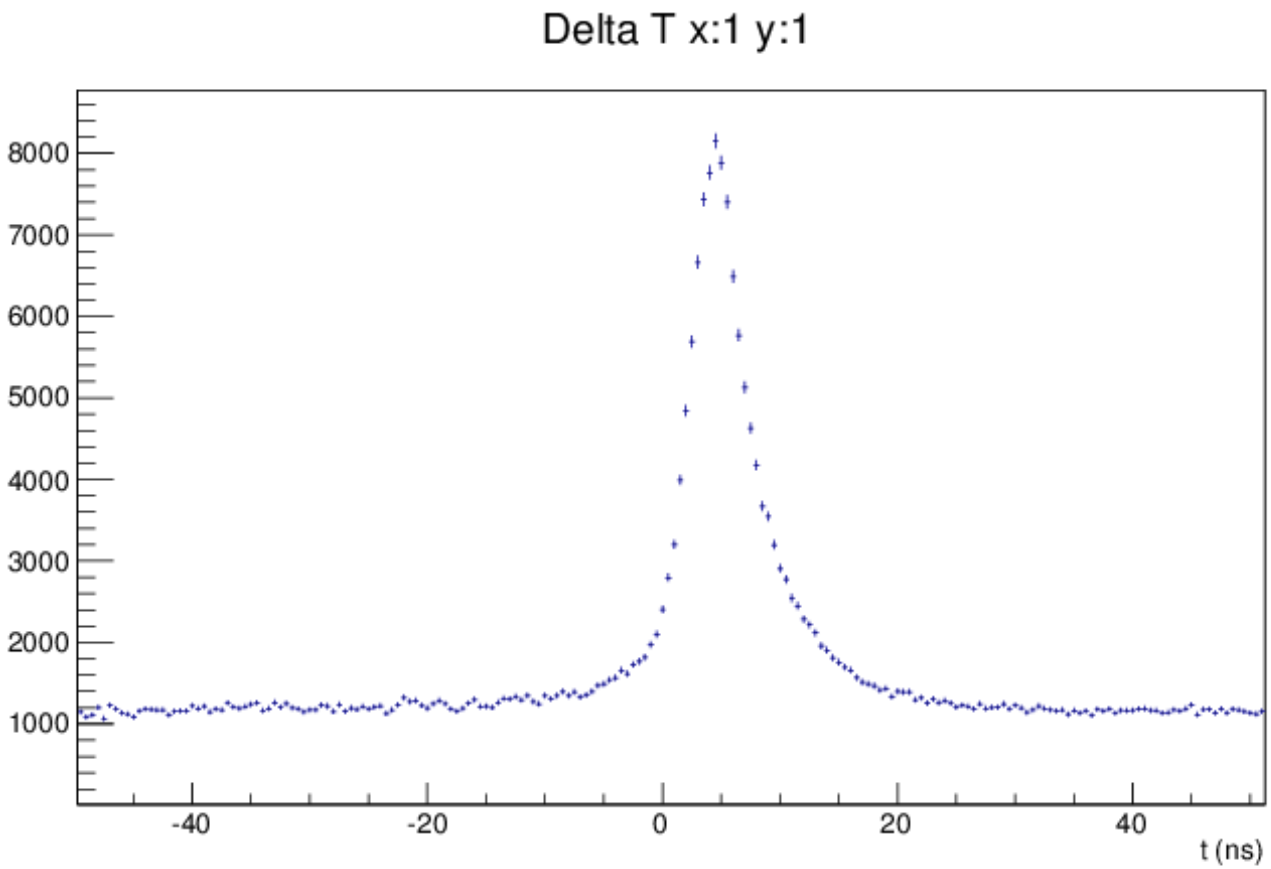

Fit function (II)

Fit function (response function) for gamma-line with energy E_i are as follows (parameters of the fit are in bold):

$$P_i(E) = \frac{1}{\sqrt{2\pi}\sigma_{\mathbf{i}}^{\mathbf{ph}}} G(E_i, \sigma_{\mathbf{i}}^{\mathbf{ph}}) + \frac{\mathbf{R_0} r^{es}(E_i)}{\sqrt{2\pi}\sigma_i^{es}} G(E_i - 511, \sigma_i^{es}) +$$
$$\frac{\mathbf{R_0} r^{es}(E_i) r^{es2}(E_i)}{\sqrt{2\pi}\sigma_i^{es2}} G(E_i - 1022, \sigma_i^{es2}) + N_i^c \mathbf{R_{Compt}} C(E_i, E)$$

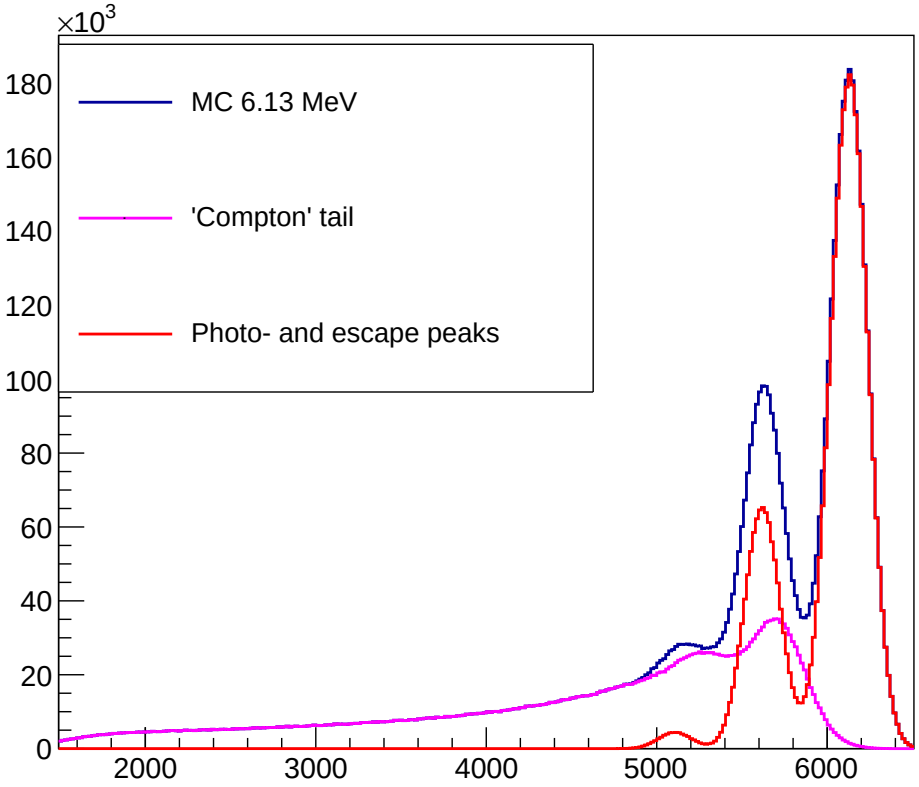

N_i - parameter which determines the amplitude of the line i in the spectrum, $\sigma_{\mathbf{i}}^{\mathbf{ph}}$ - the energy resolution for the total absorption peak for the gamma ray energy E_i. The energy resolutions σ_i^{es}, σ^{es2} depend on the resolution of $\sigma_{\mathbf{i}}^{\mathbf{ph}}$ with the law $\sigma(E_1)/\sigma(E_2) = \sqrt{E_1/E_2}$. ϵ_{ph} - total absorption peak efficiency. $r^{es}(E)$ and $r^{es2}(E_i)$ - parameters defining the amplitudes of escape peaks, normalized relatively to the amplitude of the photopeak. Dependence of the coefficient $r^{es}(E)$ и $r^{es2}(E_i)$ from the energy is set by MC, but R_0 is used to adjust them. R_{Compt} - is the factor to adjust Compton "tail" amplitude, $C(E_i, E)$ - function of Compton "tail" fucntion. $G(\bar{x}, \sigma)$ -Gauss function.

Parametrization of the “ Compton tail ”

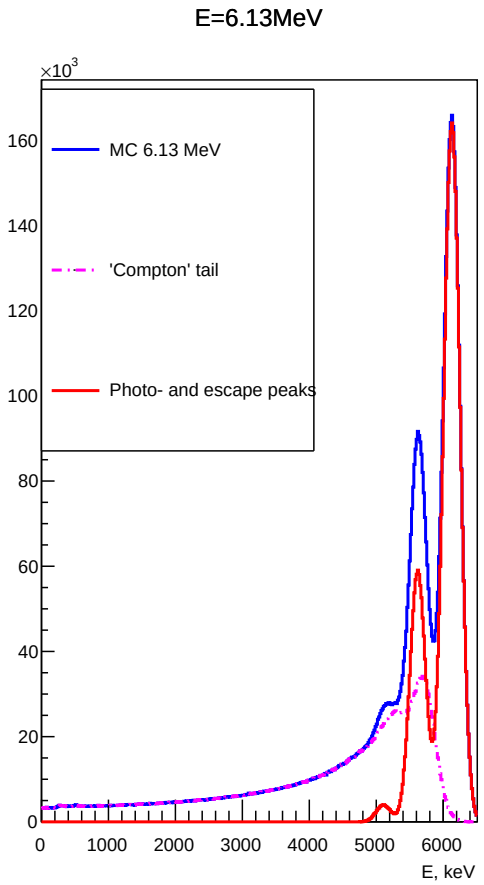

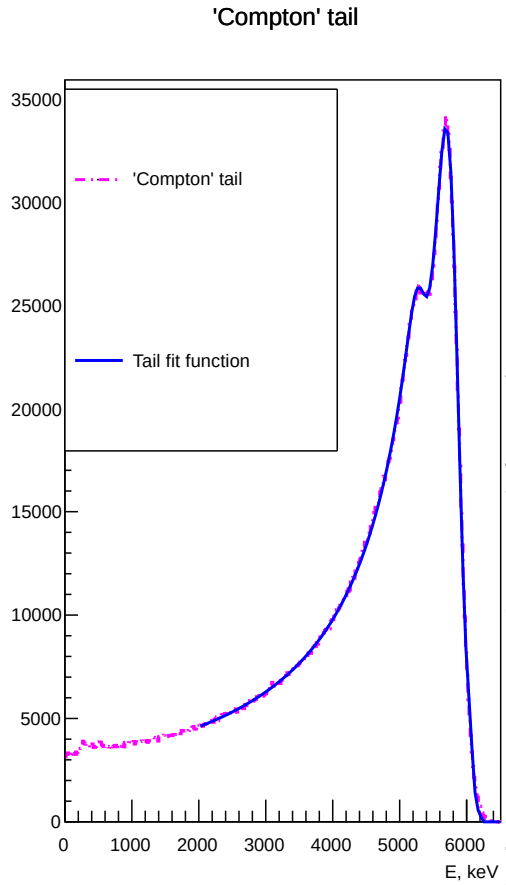

Left plot shows the response of BGO with dimensions 76x65mm for photons with energies 6.13 MeV. The blue line represents the total spectrum, the red line shows peaks of total absorption and escape peaks. Their difference (Compton “ tail ”) is shown in purple. At right plot a “ Compton tail ” and the result of the fit are shown

Function describes a single Compton scattering

$$F_1(E) = F_{1v}(E) \cdot F_{1t}(E), \qquad \textbf{where}$$

$$\mathbf{F}_{1v}(E) = P_0\, Val_0\, Erfc\left(\frac{E-(E_0-P_1)}{\sqrt{2}P_2}\right)$$

$$\mathbf{F}_{1t}(E) = e^{(E-(E_0-P_1))P_3},\ E < E_0 - P_1$$

$$\mathbf{F}_{1t}(E) = 1,\ E > E_0 - P_1$$

where Erfc - complementary error function, P_{0-3} parameters which depend on the energy of the gamma ray. A similar function for Compton scattering of annihilation photon

$$F_2(E) = F_{2v}(E) \cdot F_{2t}(E)$$

The final function has the form

$$F(E) = F_1(E) + F_2(E)$$

Parameter P_0 is normalized so that the fitting of a full range of simulated response function, the ratio of the integral of the total absorption peak to the amplitude of function $F(E)$ is equal to unity. To describe the possible deviation of this value from 1 we introduced a parameter with a range of allowd values from 0.8 to 1.3. Parameters P_2 and P_5 associated with an energy resolution of the detector.

Parametrisation of the “ Compton tail ”

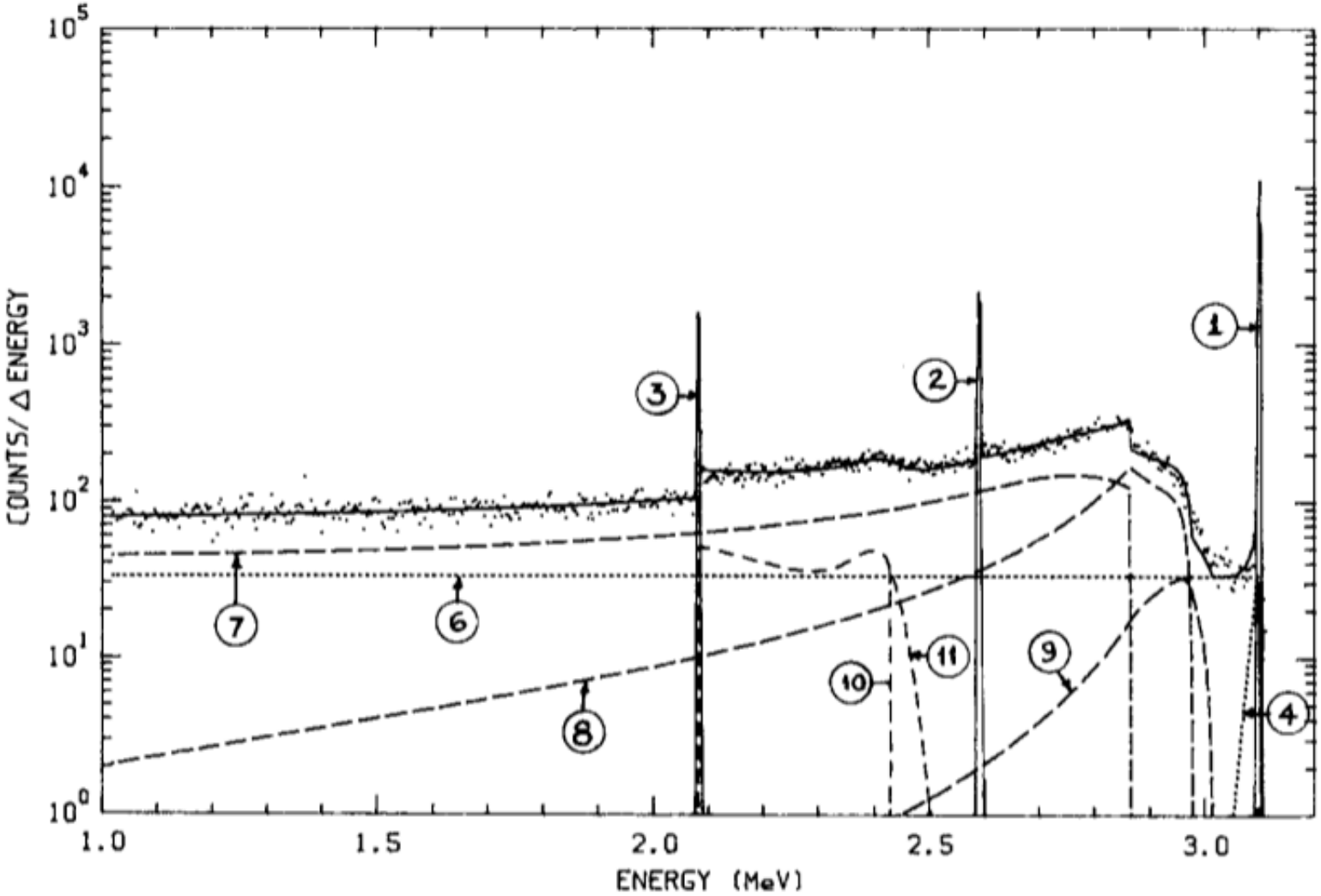

Parametrisation of the “ Compton tail ”

- 1 peak of total absorption
- 2 single escape peak
- 3 double escape peak
- 4 exponential tail peak of total absorption
- 6 flat continuum
- 7 spectrum of single Compton scattering
- 8 spectrum of double Compton scattering
- 9 triple Compton scattering spectrum
- 10 spectrum Compton of annihilation photons
- 11 spectrum of multiple scattering of annihilation photons

Description of the spectrum of the continuum

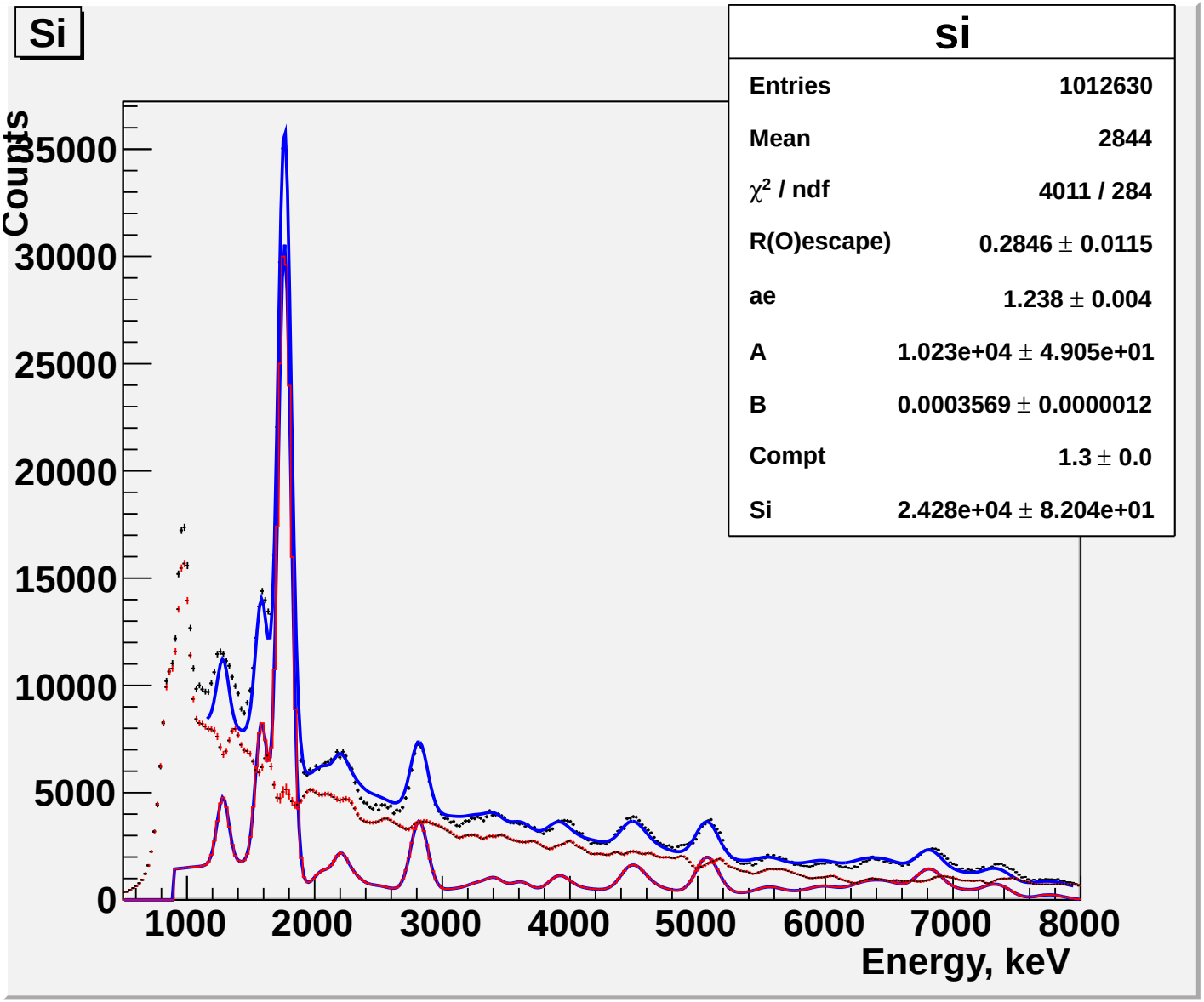

Detector DVIN-1 (II)

- The measurements were made using a portable detector DVIN-1. The detector consists of a portable neutron generator ING-27 with a built-9-alpha-pixel detector, a gamma detector on the basis of the crystal BGO, electronic data acquisition system with the alpha - and gamma - detectors, power supplies of neutron generator (NG) and alpha- and gamma- detectors.

  For detection of gamma rays produced in irradiated objects the gamma detector based on BGO crystals with a diameter of 76 mm and a thickness of 65 mm is ised. Gamma-ray detector based on BGO crystals has the following properties:

  - A good energy resolution (8-2.5%) in the energy range 1-12 MeV. On the gamma line of carbon ($E_\gamma = 4.44$ MeV) energy resolution gamma detector is about 4.4% .
  - High detection efficiency of gamma rays in this energy range.
  - A low sensitivity with respect to the registration of background neutrons.
- The time resolution of $(\alpha - \gamma)$-coincidences, is about 3.3 ns.

Detector DVIN-1 (III)

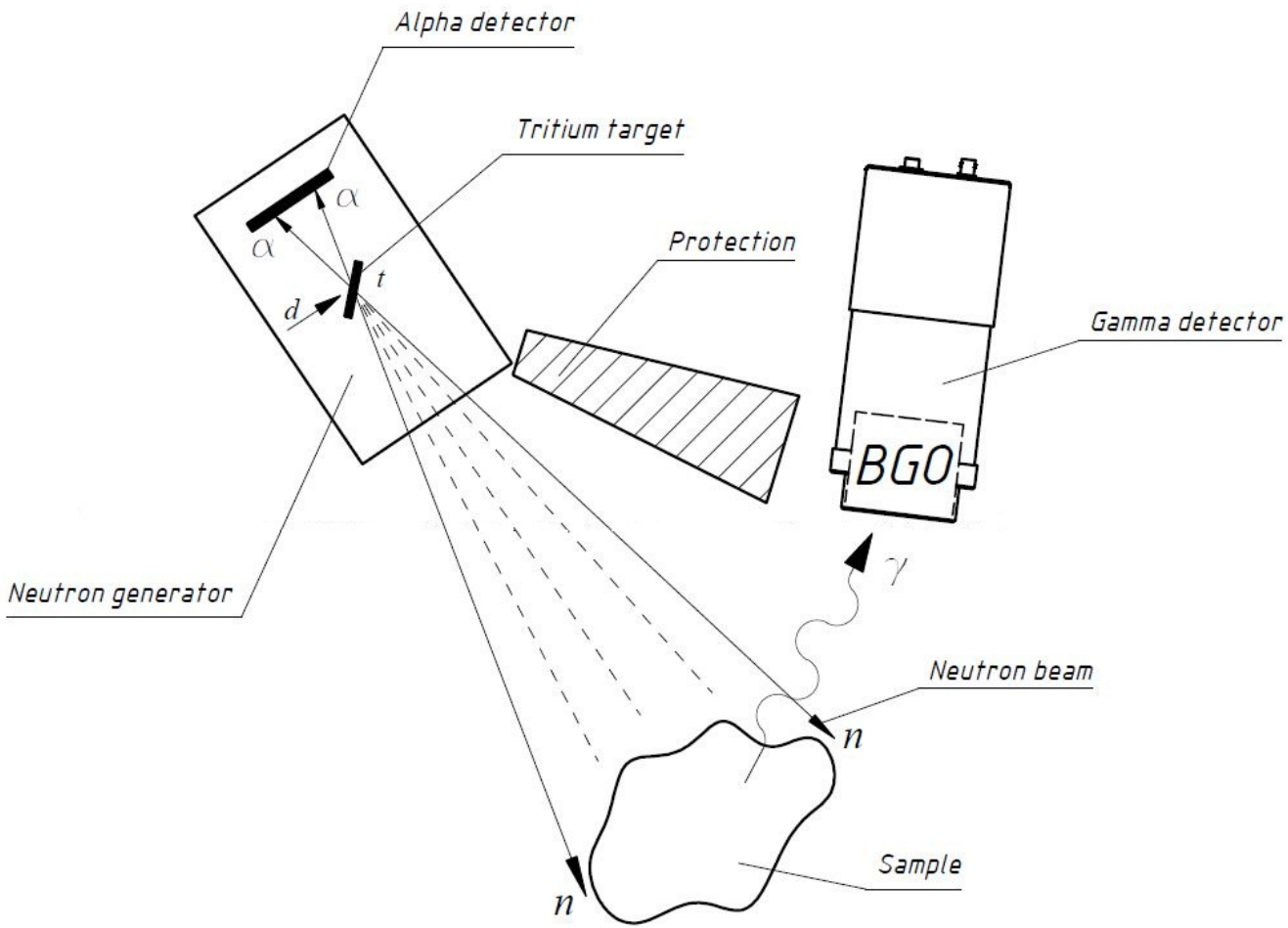

Spectrum of Fe

Gamma lines of Fe. For the case $E_\gamma > 1MeV$ and $\sigma > 4$ mBarn

Fe_2O_3

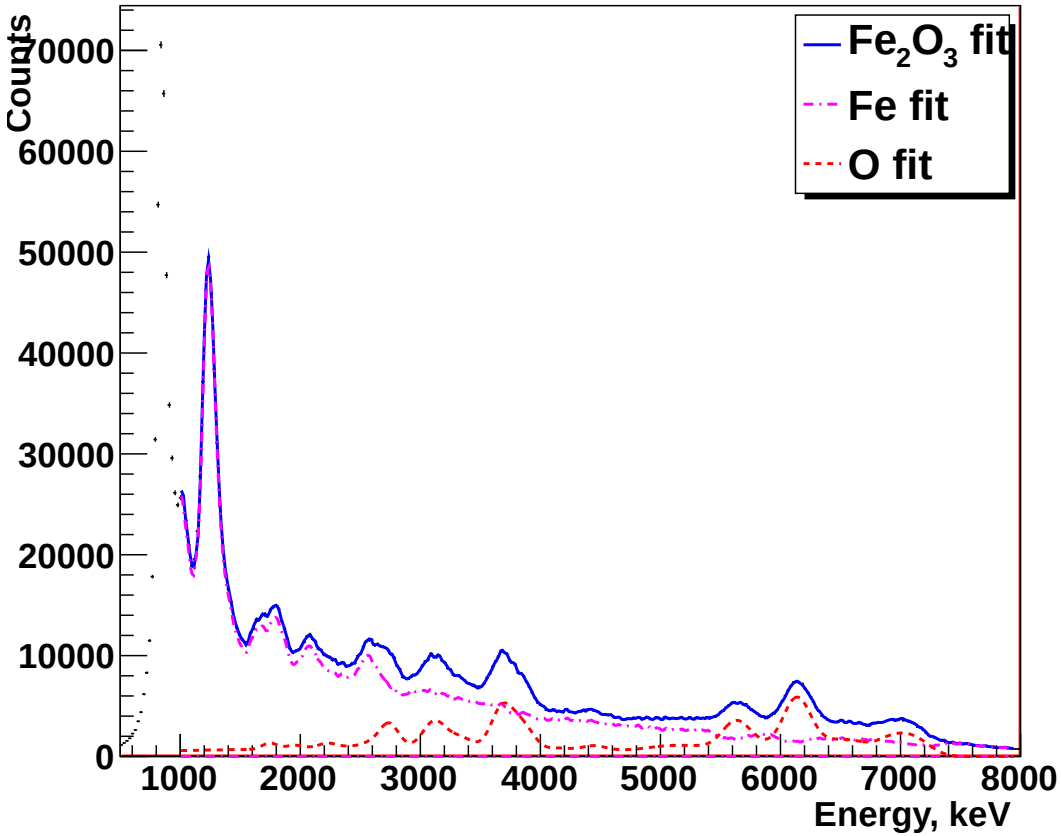

E_γ keV	σ mBarn	process
2598	35.	$(n, n' + 2n)^{56}Fe$
2523	36.	$(n, n' + 2n)^{56}Fe$
2113	41.	$(n, n' + 2n)^{56}Fe$
1811	63.	$(n, n')^{56}Fe$
1671	36.	$(n, n')^{56}Fe$
1408	50.	$(n, 2n)^{55}Fe$
1317	50.	$(n, 2n)^{55}Fe$
1305	70.	$(n, n')^{56}Fe$
1238	393.	$(n, n')^{56}Fe$
1038	82.	$(n, n')^{56}Fe$
931	126.	$(n, 2n)^{55}Fe$